Charge Translocation by the Na^+/K^+ Pump under Na^+/Na^+ Exchange Conditions: Intracellular Na^+ Dependence

Miguel Holmgren* and Robert F. Rakowski†
*National Institutes of Health, National Institute of Neurological Disorders and Stroke, Bethesda, Maryland; and †Department of Biological Sciences, Ohio University, Athens, Ohio

ABSTRACT The effect of intracellular (i) and extracellular (o) Na^+ on pre-steady-state transient current associated with Na^+/Na^+ exchange by the Na^+/K^+ pump was investigated in the vegetal pole of *Xenopus* oocytes. Current records in response to 40-ms voltage pulses from −180 to +100 mV in the absence of external Na^+ were subtracted from current records obtained under Na^+/Na^+ exchange conditions. Na^+-sensitive transient current and dihydroouabain-sensitive current were equivalent. The quantity of charge moved (Q) and the relaxation rate coefficient (k_{tot}) of the slow component of the Na_o^+-sensitive transient current were measured for steps to various voltages (V). The data were analyzed using a four-state kinetic model describing the Na^+ binding, occlusion, conformational change, and release steps of the transport cycle. The apparent valence of the Q vs. V relationship was near 1.0 for all experimental conditions. When extracellular Na^+ was halved, the midpoint voltage of the charge distribution (V_q) shifted -25.3 ± 0.4 mV, which can be accounted for by the presence of an extracellular ion-well having a dielectric distance $\delta = 0.69 \pm 0.01$. The effect of changes of Na_i^+ on Na_o^+-sensitive transient current was investigated. The midpoint voltage (V_q) of the charge distribution curve was not affected over the Na_o^+ concentration range 3.13–50 mM. As Na_i^+ was decreased, the amount of charge measured and its relaxation rate coefficient decreased with an apparent K_m of 3.2 ± 0.2 mM. The effects of lowering Na_i^+ on pre-steady-state transient current can be accounted for by decreasing the charge available to participate in the fast extracellular Na^+ release steps, by a slowly equilibrating (phosphorylation/occlusion) step intervening between intracellular Na^+ binding and extracellular Na^+ release.

INTRODUCTION

Studies of transient current associated with the Na^+/K^+ pump

Nakao and Gadsby (1) were the first to report pre-steady-state transient current associated with the Na^+/K^+ pump in the absence of K^+ in cardiac myocytes. The strophanthidin-sensitive difference current elicited by voltage jumps requires the presence of intracellular ATP and Na^+, and is blocked by oligomycin B. The amount of charge translocated (measured as the integral of the transient current) has a sigmoid voltage-dependence that can be described by a Boltzmann distribution with an apparent valence (z) of 1.0 appropriate for a single positive charge moved through the entire membrane field. The voltage-dependence of transient current has also been studied in intact (2) and cut-open *Xenopus* oocytes (3). Dihydroouabain- (DHO) and Na_o^+-sensitive transient currents measured in K^+-free internal and external solutions were shown to be similar in their voltage-dependence and kinetic properties. The transient current is dependent on the presence of intracellular Na^+ and nucleotides, and is diminished by activation of forward Na^+/K^+ pumping, by addition of extracellular K^+ or by addition of 10 μg ml^{-1} oligomycin B. The voltage-dependence of the steady-state charge distribution and the relaxation rate coefficient of the transient current can be described by a simple two-state model in which only the reverse rate coefficient is voltage-dependent. Time-resolution of current obtained with the two-microelectrode and cut-open oocyte techniques is limited by the rise time of the voltage steps that can be achieved. Rettinger et al. (4) obtained improved temporal resolution using the patch-clamp technique and Hilgemann (5) was able to separate the transient current recorded from cardiac myocytes into two components using the giant patch technique. The highest temporal resolution of the transient current has been obtained in squid giant axons in which it was possible to demonstrate the existence of three current components that are thought to correspond to the sequential release of three Na^+ ions to the extracellular solution (6).

Lack of data on the effects of intracellular Na^+ on charge movement in cellular preparations

A relatively large number of studies have been published that were restricted to the examination of deocclusion and extracellular Na^+ release steps by limiting the availability of ADP and by operating at saturating Na_i^+ in *Xenopus* oocytes, squid giant axons, and cardiac myocytes (2,6,7). No previous work in a cellular preparation has been published that examines the effect of changes in Na_i^+ on transient current by the Na/K pump. On the other hand, intracellular effects on charge translocation have been extensively studied in non-cellular systems. Intracellular Na^+ binding has been studied in proteoliposomes (8,9) and in Na^+,K^+-ATPase-containing membrane fragments adsorbed onto lipid bilayers (10,11).

Submitted August 22, 2005, and accepted for publication November 14, 2005.
Address reprint requests to R. F. Rakowski, Tel.: 740-593-2330; Fax: 740-593-0300; E-mail: rakowski@ohio.edu.

0006-3495/06/03/1607/10 $2.00
doi: 10.1529/biophysj.105.072942

These studies have led to the hypothesis that intracellular Na^+ binding to the Na^+/K^+ pump has a dielectric coefficient of ~0.25. The first two Na^+ ions are thought to bind to two negatively charged sites, and to do so in an electroneutral fashion. All of the charge movement associated with intracellular Na^+ binding has been ascribed to the binding of the third ion to an Na^+-selective site in a shallow internal ion-well (12,13).

Postulated effect of intracellular Na^+ on transient current

In this report, we examine the effect of extracellular and intracellular Na^+ on pre-steady-state charge translocation mediated by the Na^+/K^+ pump in oocytes in which the internal solution composition was controlled by direct perfusion or by equilibration across a region of membrane permeabilized with saponin. Rather than restricting the partial reactions of the pump cycle to only those associated with deocclusion and release of Na^+ at its external face, we wished to examine the ability of Na_i^+ to increase the amount of charge deoccluded and released from the external face of the enzyme. The experiments described here were performed in the presence of 5 mM internal ATP and ADP. This promotes electroneutral Na^+/Na^+ exchange by permitting the slow reverse reaction step, resulting in phosphorylation of ADP to ATP. In these conditions, both the forward and reverse steps that are associated with binding and occlusion of Na^+ at the internal side of the enzyme can occur. This should allow equilibration of internal Na^+ with its occlusion sites and thus make additional Na^+ available for release in response to a depolarizing voltage pulse. The experiments described below are designed to test this postulated effect of Na_i^+ on pre-steady-state current.

MATERIALS AND METHODS

Preparation and incubation of oocytes

Oocyte-positive, adult female African clawed frogs (*Xenopus laevis*) were obtained from *Xenopus* I (Ann Arbor, MI) and were maintained on a high protein diet in freshwater tanks. The methods of dissection, enzymatic treatment, and incubation of oocytes have been described previously (13,14). Oocytes were stored at 17°C in Barth's solution with 50 μg ml^{-1} streptomycin and 50 units ml^{-1} penicillin. The Barth's solution had the following composition: 88 mM NaCl, 3 mM KCl, 2.4 mM $NaHCO_3$, 0.82 mM $MgSO_4$, 0.33 mM $Ca(NO_3)_2$, 0.41 mM $CaCl_2$, and 5 mM Tris HEPES (pH = 7.1).

Experimental solutions

100 Na, 0 K external solution had the following composition: 100 mM Na sulfamate, 20 mM tetraethylammonium (TEA) sulfamate, 3 Mg sulfamate, 5 mM $Ba(NO_3)_2$, 2 mM $Ni(NO_3)_2$, 0.01 mM $Gd(NO_3)_3$, 0.3 mM niflumic acid, and 10 mM Tris HEPES (pH = 7.6). The 0 Na 0 K external solution was obtained by equimolar substitution of tetramethylammonium for Na^+. Intermediate extracellular Na^+ concentrations were obtained by mixing 100 Na 0 K and 0 Na 0 K solutions. The composition of the internal solution was 50 mM Na sulfamate, 20 mM TEA sulfamate, 10 mM $MgSO_4$, 5 mM MgATP, 5 mM TrisADP, 5 mM 1,2-bis(2-aminophenoxy)ethane-N,N,N′,N′-tetraacetic acid, 30 mM N-methyl D-glucamine (NMDG) sulfamate, and 10 mM Tris HEPES (pH = 7.3). Na^+-free internal solution was prepared by equimolar substitution of NMDG for Na^+. Intermediate intracellular Na^+ concentrations were obtained by mixing internal solutions containing 50 and 0 mM Na^+. Note that both ATP and ADP were present in the intracellular solution to promote electroneutral Na^+/Na^+ exchange (15,16). The solutions were designed to minimize non-pump-mediated current. Extracellular TEA^+ (20 mM) was present to block passive K^+ conductance (3,17). NMDG was used as an internal Na^+ substitute in the expectation that it would be less likely to compete for Na^+ binding sites than smaller cations. The solutions were nominally chloride-free and were also Ca^{2+}-free to prevent activation of Ca^{2+}-dependent anionic current. Ni^{2+} and Gd^{3+} were present to block Na^+/Ca^{2+} exchange (18) and stretch-activated cation channels (19), respectively.

Electrophysiological measurements

Two modifications (internal perfusion and saponin permeabilization) of the open-oocyte, guarded-seal technique (20) were used to study the effect of intracellular and extracellular Na^+ on transient current mediated by the Na^+/K^+ pump. The effect of changes in Na_i^+ was studied in internally perfused oocytes as described previously (3,21). Internal perfusion was performed through a glass micropipette (internal diameter of 0.58 mm and length of ~1 cm) that injected solution at a rate of 50–60 μl h^{-1}. On the other hand, because longer duration experiments could be performed, the effect of changes in Na_o^+ was also studied in permeabilized oocytes. After the cell was mounted with its (dark) animal pole oriented toward the intracellular compartment of the experimental chamber, it was permeabilized by adding 0.1% saponin to the intracellular compartment. Permeabilization resulted in a decrease in access resistance and large increase in total capacitance that resulted in an increase in the time constant of small amplitude (10–20 mV) test voltage-clamp pulses. Permeabilization required from 3 to 10 min, after which the solution was replaced by the experimental intracellular solution and allowed to equilibrate for an additional period of time (10–30 min) until there was no change in steady-state or transient current magnitude. Permeabilization with saponin permitted stable electrical recording for more than 2 h. Internally perfused oocytes were not as stable as permeabilized oocytes, but allowed changes of internal solution to be made whereas equilibration at various Na_i^+ was too slow to be practical in permeabilized oocytes. Since both the charge relaxation rate coefficients and the total charge moved (Q_{tot}) obtained with perfused oocytes were in agreement with those obtained after saponin treatment, we conclude that saponin treatment has no effect on the transient currents measured in this study.

The voltage-clamp system was obtained from DAGAN (Model CA-1 High Performance Oocyte Clamp; Minneapolis, MN). The holding potential was −40 mV. Voltage pulses from 30 to 40 ms in duration were made from the holding potential to command potentials over the range −180 to +100 mV in increments of 20 mV. Pulses were applied every 500 ms. The current records were obtained by averaging 12–20 repetitions of the pulse protocol. Data were acquired using an analog-to-digital converter system and software (TL-1 DMA interface, 100 KHz, PCLAMP version 6; Molecular Devices, Sunnyvale, CA) running on an IBM-compatible computer system (Dell Computer, Austin, TX). The analog signal was filtered at 2–5 KHz before being digitized, and was sampled every 66 μs.

Difference current was calculated by subtraction of the current records obtained after halting Na^+/Na^+ exchange by addition of 20 μM DHO or removal of Na_o^+ from records acquired just before stopping the exchange (3). Despite the presence of the various channel blocking agents, a steady-state (leakage) current was still observed. Part of the leakage current may arise owing to imperfect electrical isolation by the guard compartment. In some experiments, a time-dependent increase in steady-state leakage current also required subtraction. The rate of increase of the leakage current was sufficiently slow, however, that it could be treated as time-independent during the voltage pulses. The integral and relaxation rate coefficient of the transient

current were determined using CLAMPFIT software modules of PCLAMP 6.0. The Na_o^+- or DHO-sensitive transient current was preceded by a fast component with a time course close to that of the voltage step (relaxation rate >2000 s^{-1}). Therefore, the transient current was fit with the sum of two-exponential relaxation rate coefficients, but only the relaxation rate coefficient of the slow component was analyzed further. The integral of the slow component was determined by direct numerical integration of the subtracted current records over a 35-ms time period starting 400–800 μs after the start of the voltage step. The integral of the fast component was not calculated. Further analysis, least-squares curve fitting, and preparation of figures were done with SIGMAPLOT software (Systat Software, Richmond, CA). Curve fit parameters are reported means ± SE of the value obtained from the least-squares fitting procedure. Experiments were performed at room temperature (~22°C).

RESULTS

Kinetic model for internal Na^+ occlusion and extracellular Na^+ release

A pseudo-three-state kinetic model of reaction steps that are presumed to occur between the Na^+-occluded, ADP-bound form of the enzyme ($(Na_3)E_1P\cdot ADP$) and the release of 3 Na^+ to the extracellular space from the E_2P form of the enzyme (Reaction Scheme 1) has been described in detail by Peluffo (22):

Reaction Scheme 1

$$(Na_3)E_1P\cdot ADP \underset{\kappa_{-1}}{\overset{k_1}{\rightleftharpoons}} (Na_3)E_1P \underset{\kappa_{-2}}{\overset{k_2}{\rightleftharpoons}} E_2P + 3Na_o.$$

The first-order rate constant k_1 describes the Na_i^+ and voltage-independent release of ADP from the left-most intermediate. The parameter κ_{-1} is a pseudo-first-order rate coefficient describing the rebinding of ADP, defined by the following equation: $\kappa_{-1} = k_{-1}[ADP]$, where k_{-1} is a second-order rate coefficient and [ADP] is the intracellular ADP concentration. The value of k_{-1} measured by Peluffo (22) was 6.89×10^4 s^{-1} M^{-1}. Since all of the experiments described here were done at 5 mM [ADP], a value of κ_{-1} of 345 s^{-1} is used in all of the least-squares curve-fitting calculations described below in which this rate coefficient is explicit rather than lumped with others. The rate coefficient κ_{-2} is a voltage- and Na_o^+-dependent rate coefficient that describes extracellular Na_o^+ rebinding and occlusion. Its relationship to other parameters can be written as

$$\kappa_{-2} = k_{-2}[Na]_o^n \exp(-zFV_m/RT), \quad (1)$$

where k_{-2} is a voltage-independent rate coefficient that combines extracellular Na^+ rebinding and occlusion as well as the conformational change E_2P to E_1P. The expression $[Na]_o^n \exp(-zFV_m/RT)$ accounts for Na^+ ion rebinding within an extracellular access channel. The parameter n in this equation is the apparent molecularity of the charge-moving process, as described below. The rate coefficient k_2 describes the E_1P–E_2P conformational change accompanied by Na^+ deocclusion followed by rapid release of 3 Na^+ to the extracellular space. In principle, the release steps should also be voltage-dependent, since they are postulated to occur within the same extracellular ion-well as the Na^+-rebinding steps described by Eq. 1. However, for the sake of simplicity, it is assumed that the voltage-dependence of Na^+ release can be ignored, since those steps occur after the relatively slow E_1P–E_2P conformational change with which they have been lumped. This simplification was found to be acceptable in previous work (2,22), and is likely to hold true, except at very negative membrane potentials, which would slow the extracellular Na^+ release steps so they are comparable in rate to the deocclusion step. Attempts to include the voltage-dependence of extracellular Na^+ release in Scheme 1 showed that a shallow minimum would be produced in the k_{tot} vs. V relationship. This behavior has been observed in preliminary experiments at very low Na_o^+ but has not been investigated in detail.

Effect of extracellular Na^+ on the pre-steady-state Q vs. V relationship

Fig. 1 *A* shows Na_o^+-sensitive difference current records from an oocyte bathed in 100 mM Na^+. The records are the subtracted average of 20 current transients elicited by voltage-clamp pulses measured before and after removal of Na_o^+. Additional data were recorded from this oocyte at 50, 25, and 12.5 mM Na_o^+. At the end of the experiment the extracellular solution was changed back to 100 mM Na^+ and DHO-sensitive current transients were measured that were comparable to those shown in Fig. 1 *A* (*open triangles* in Fig. 1, *B* and *E*). A similar comparison of Na_o^+- and DHO-sensitive difference current at 100 mM Na_o^+ has been made previously (3).

The difference current records in Fig. 1 *A* have two components—a fast component (truncated at this gain) that has a time course similar to the rise-time of the voltage step (400–600 μs), and a slow component whose relaxation rate coefficient is voltage-dependent. Holmgren et al. (6) have been able to further separate the fast component in experiments on squid giant axons and have shown that there are three distinct sequential steps in the release of Na^+ that are postulated to correspond to the deocclusion and release of each of the three translocated Na^+ ions. The temporal resolution of the present experiments, however, was insufficient to resolve the fast components. We, therefore, restrict our analysis to the slow component. The integral of the slow component during the *on* (Q_{on}) for the records in Fig. 1 *A* and similar records obtained at various Na_o^+ was normalized by dividing by its respective value of Q_{tot}. The resulting data are plotted in Fig. 1 *B*.

Alternative Q vs. V relationships for Scheme 1

The normalized pre-steady-state charge distribution $(Q(V) - Q_{min})/Q_{tot}$ for Scheme 1 can be written in several forms. The traditional (Boltzmann) form of the charge distribution is given by Eq. 2,

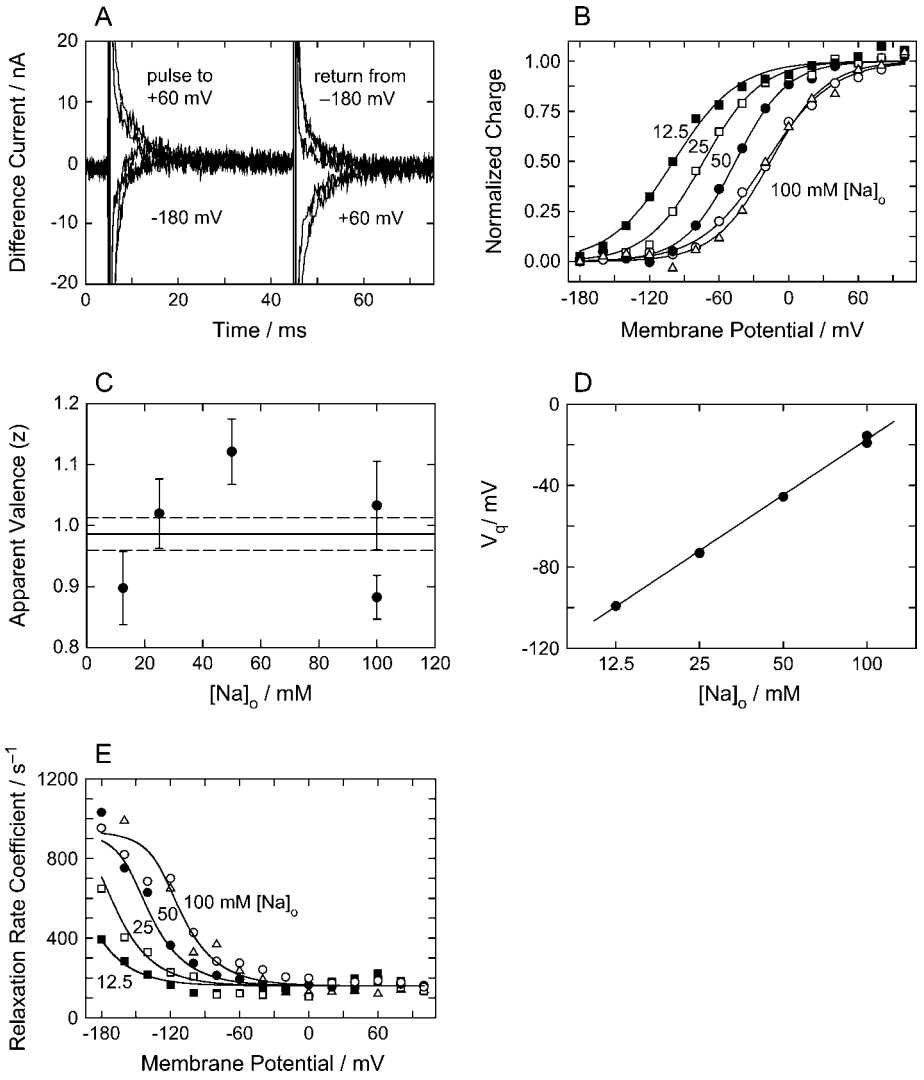

FIGURE 1 Extracellular Na^+-sensitive current transients from a permeabilized oocyte equilibrated with 50 mM intracellular Na^+. (*A*) Averaged current records are shown for Na_o^+ = 100 mM. Voltage-clamp pulses, 40-ms in duration, were done in increments of 20 mV from −180 to +100 mV from a holding potential of −40 mV. The Na_o^+-sensitive difference current for each voltage was determined by subtraction of 20 records obtained after removal of Na^+ from 20 in its presence. For clarity, only the five difference current records elicited by voltage-clamp pulses to −180, −120, −60, 0, and +60 mV are shown. The sequence of changes to nonzero values of Na_o^+ in experiments of this kind was performed in random order. In this experiment, the sequence was 100, 0, 50, 0, 12.5, 0, 25, 0, and then again 100 mM Na_o^+, followed by addition of 20 μM DHO. (*B*) Voltage-dependence of the normalized charge moved during the *on* (Q_{on}). *Open circles* and *triangles* correspond to data from the beginning and end of the experiment, respectively, at an Na_o^+ of 100 mM. Other data measured at 50 mM (*solid circles*), 25 mM (*open squares*), and 12.5 mM (*solid squares*). The solid lines are least-square fits of Eq. 2 to Q_{on} for the data at various Na_o^+ values. The data were normalized by subtraction of Q_{min} and dividing by the total charge (Q_{tot}) determined at 100 mM Na_o^+ from a preliminary fit to a nonnormalized version of Eq. 2. (*C*) The least-squares values of z, mean ± SE, from the fits obtained in *B* are plotted as a function of Na_o^+ (*solid circles*). The data in *B* were also fit simultaneously to Eq. 4. The best-fit values were $z = 0.99 \pm 0.03$, $n = 1.56 \pm 0.06$, and $A = 18.2 \pm 2.7\ M^{-1}$. The solid and dashed lines in *C* represent the least-squares value of z, mean ± SE, respectively, from this simultaneous fit. (*D*) The least-squares values of V_q determined from the individual fits in *B* are plotted at each Na_o^+ (*solid circles*). The mean ± SE is smaller than the diameter of the symbols. The solid line is calculated according to Eq. 5 with the best-fit values of z, n, and A determined in *B*. (*E*) Voltage-dependence of the slow charge relaxation rate coefficient (k_{tot}). Open and solid symbols as in *B*. For each concentration, the value shown at −40 mV was obtained by averaging the data from the off-transients. The mean ± SE for the data at −40 mV is smaller than radius of the symbols. The solid lines are the least-squares fit of Eqs. 1 and 6, with the value of κ_{-1} set to 345 s^{-1}, and $K_m(0)$ set to 3.2 mM. The parameter values obtained from the fit were $k_1 = 597 \pm 22\ s^{-1}$, $k_2 = 287 \pm 14\ s^{-1}$, and $k_{-2} = 221 \pm 14\ s^{-1}\ M^{-1}$. The data shown in *A–E* were obtained from the same oocyte.

$$\frac{Q(V) - Q_{min}}{Q_{tot}} = \frac{1}{1 + \exp\left[\frac{zF(V_q - V)}{RT}\right]}, \tag{2}$$

where Q_{tot} is the total available amount of moveable charge, Q_{min} is the minimum value of charge approached at extreme negative voltages, z is the apparent valence of the charge, V_q is the midpoint voltage of the charge distribution, V is the membrane potential during the test voltage step, and F, R, and T have their usual meanings. The solid lines in Fig. 1 *B* are the best fits of Eq. 2 to the data at each Na_o^+. Equation 2 can be written in an alternative form that accounts for the effect of changes in Na_o^+, as follows. For Scheme 1, the midpoint voltage V_q is defined by Eq. A10 of Peluffo (22) and is given here slightly modified as Eq. 3:

$$\left(\frac{1}{k_2} + \frac{\kappa_{-1}}{k_1 k_2}\right) k_{-2} [Na]_o^n = \exp\left(\frac{zFV_q}{RT}\right). \tag{3}$$

Substitution of Eq. 3 in Eq. 2 gives the expression for the Q vs. V relationship of

$$\frac{Q(V) - Q_{min}}{Q_{tot}} = \frac{1}{1 + A[Na]_o^n \exp\left(\frac{-zFV}{RT}\right)}, \tag{4}$$

where $A = k_{-2}(k_1 + \kappa_{-1})/k_1 k_2$. Rearranging Eq. 3, we obtain the following expression for V_q:

$$V_q = \frac{RT}{zF} \ln(A[Na]_o^n). \tag{5}$$

The apparent valence (z) is independent of Na_o^+

The solid circles in Fig. 1 *C* (mean ± SE) are the values of the apparent valence (z) determined by the least-squares fit of Eq. 2 to the data at each Na_o^+ in *B*. The value of z obtained from the simultaneous fit of all of the data in Fig. 1 *B* to Eq. 4 is shown as the solid line (mean ± SE, *dashed lines*) in Fig. 1 *C*. There is no obvious dependence of z on Na_o^+ and its value is close to 1.0. In this study, curve fits that included the parameter z were performed initially with z as a free parameter. Since the mean value of z was found to be not-significantly-different from 1.0, it was simply set equal to 1.0 for subsequent fits. Previous measurements of pre-steady-state transient current in intact oocytes (2) or oocytes internally perfused with ADP (3,22) are also consistent with a value of $z = 1.0$.

Extracellular Na^+ dependence of the midpoint voltage (V_q)

The values of V_q determined from the least-squares fit of Eq. 2 to the data in *B* at each Na_o^+ are plotted in Fig. 1 *D*. The solid line is drawn according to Eq. 5, using the parameters determined from the simultaneous fit of Eq. 4 to the entire data set in *B*. The parameters z and n in Eqs. 3–5 are related by the expression: $z = nq\delta$ (23), where q is the charge of the translocated species (+1.0 for Na^+) and δ is the fractional distance that it moves through the membrane field. The two alternative methods of fitting the Q vs. V data in *B* (Eqs. 2 and 4) gave identical values of $z = 0.99 \pm 0.03$ for both methods and $n = 1.56 \pm 0.06$ from Eq. 4. From these values, we calculate a value of $\delta = 0.63 \pm 0.05$. This is consistent with various estimates of the dielectric coefficient for extracellular Na^+ release (e.g., 0.65) (11). An additional calculation based on a summary of all such data in this study is given in Fig. 2 below.

Voltage-dependence of the relaxation rate coefficient for Scheme 1

Scheme 1 does not attempt to separate the kinetics of extracellular Na^+ rebinding into individual components for each Na^+ ion or to consider the voltage-dependence of the extracellular Na^+ release steps. The rate coefficient κ_{-2} in Scheme 1 describes a lumped extracellular Na^+ rebinding process and includes the E_2P–E_1P conformational change. Three eigenvalues are expected to describe the transient behavior of Scheme 1. One eigenvalue is zero. The other two are obtained from the two real roots of a quadratic expression. The eigenvalue of interest is the one associated with the negative root since the requirement that the rate coefficients be positive means that the negative root will be the smaller of the two, and therefore will govern the slow rate coefficient of charge relaxation. The voltage-dependence of the rate coefficient for slow-charge relaxation (k_{tot}) is shown for various Na_o^+ in Fig. 1 *E*. The relaxation-rate coefficient of the slow component is given by Eq. 6, which is the negative root of the quadratic expression obtained for Scheme 1 (see (22)):

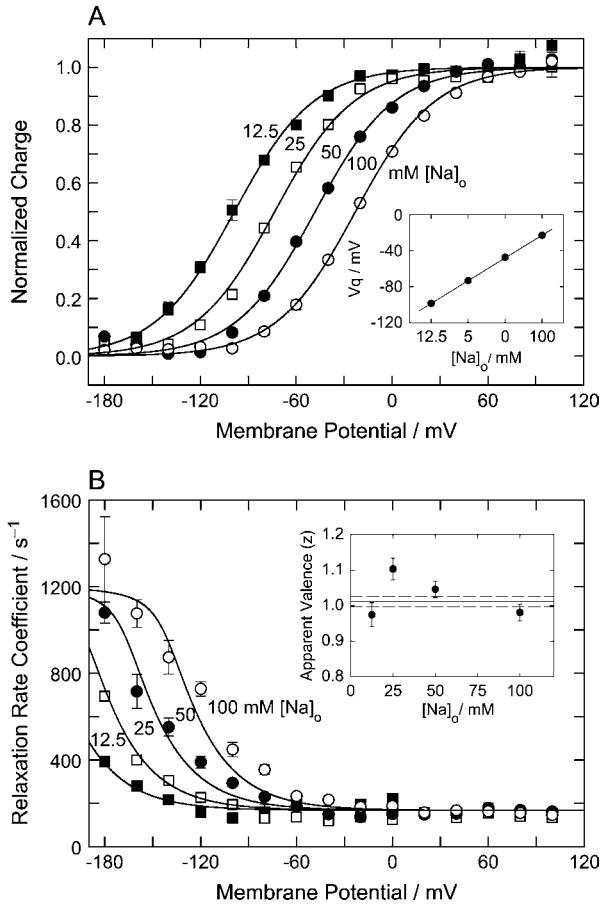

FIGURE 2 Effect of Na_o^+ on the voltage-dependence of extracellular Na^+-sensitive charge and current relaxation rate coefficient in permeabilized oocytes equilibrated with solutions containing 50 mM Na_o^+. The data were obtained from seven oocytes in which the extracellular Na^+-sensitive Q_{on} was determined at 100 mM Na_o^+ and at least at one other concentration. (*A*) Voltage-dependence of the normalized charge at 100 mM Na_o^+ (*open circles*, $N = 9$, where N is the number of measurements made at this concentration), 50 mM (*solid circles*, $N = 5$), 25 mM (*open squares*, $N = 3$), and 12.5 mM (*solid squares*, $N = 3$). Solid lines are calculated from a least-squares fit of Eq. 4 to the data. The best-fit values for the parameters were $z = 1.01 \pm 0.01$, $n = 1.47 \pm 0.03$, and $A = 11.8 \pm 0.9$. The data from each oocyte at each Na_o^+ were normalized by subtraction of Q_{min} and dividing by the value of total charge (Q_{tot}) determined by a preliminary fit of $Q(V)$ from Eq. 2 to the data at each Na_o^+. (*Inset*) Solid circles are the values of V_q obtained from fits of Eq. 2 to the data at each Na_o^+. The solid line is calculated according to Eq. 5 with the best-fit values of z, n, and A given above. (*B*) Voltage-dependence of the charge relaxation rate coefficient (k_{tot}) of Na_o^+-sensitive current at various Na_o^+. Symbols correspond to those in *A*. The solid lines are least-squares fits of Eqs. 1 and 6 to the data with the value of κ_{-1} set to 345 s^{-1}. The best-fit parameters were $k_1 = 852 \pm 31$ s^{-1}, $k_2 = 252 \pm 13$ s^{-1}, and $k_{-2} = 113 \pm 6$ s^{-1} M^{-1}. (*Inset*) Solid circles are the values of z mean ± SE determined from the fit of Eq. 2 to the $Q(V)$ data in *A*. The least-squares value of z, mean ± SE, from the fit of the data in *A* to Eq. 4 is shown as the solid and dashed lines, respectively. For the entire figure, the mean ± SE is smaller than the size of the symbol if no error bar is visible.

$$k_{tot} = 0.5\left[k_1 + \kappa_{-1} + k_2 + \kappa_{-2} - \sqrt{(k_1 + \kappa_{-1} + k_2 + \kappa_{-2})^2 - 4[k_1k_2 + (k_1 + \kappa_{-1})\kappa_{-2}]}\right]. \quad (6)$$

Summary of the effect of changes in extracellular Na^+ in oocytes equilibrated with 50 mM intracellular Na^+

Fig. 2 is a summary of the data obtained from seven oocytes in which Na_o^+-sensitive transient current was initially measured in 100 mM Na_o^+ and subsequently in at least one other Na_o^+. The oocytes were permeabilized with saponin and exposed to 50 mM Na_i^+. The least-squares fit of Eq. 4 to the data in *A* gave values of $z = 1.01 \pm 0.01$ and $n = 1.47 \pm 0.03$. This corresponds to a value of δ of 0.69 ± 0.02 corresponding to a shift of the midpoint voltage of -25.3 ± 0.4 mV for each halving of Na_o^+, values that are consistent with previous measurements in oocytes and squid giant axon (24,25). The inset in Fig. 2 *A* shows V_q determined from individual fits of Eq. 2 (*solid circles*). The solid line is a plot of V_q calculated from Eq. 5 using the parameters from the simultaneous fit of the data in *A* to Eq. 4. The mean values of the relaxation rate coefficient of slow charge (k_{tot}) measured in these seven oocytes at various Na_o^+ are plotted in Fig. 2 *B*. The solid lines are calculated from the least-squares fit of Eqs. 1 and 6 to the data using the parameters given in the figure legend. The solid circles in the inset are the values of z (mean $\pm$ SE) from the individual fits to Eq. 2 to the data in Fig. 2 *A*. The solid and dashed lines show the value of z (mean $\pm$ SE) obtained from the fit of Eq. 4 to the data in *A*.

Effect of intracellular Na^+ on the availability of pre-steady-state charge

The following kinetic model can be written to describe equilibrium binding of intracellular Na^+ ions to the E_1ATP conformation of the enzyme. The electrogenic binding of Na^+ within a shallow internal ion-well is expected to occur very rapidly compared to a subsequent slow occlusion reaction (13). We assume that these steps can be lumped as a single reaction step governed by a holding-potential dependent equilibrium coefficient ($K_m(V_h)$). See Scheme 2, below:

Reaction Scheme 2

$$3Na_i + E_1ATP \overset{K_m(V_h)}{\leftrightarrow} (Na_3)E_1P \cdot ADP \underset{\kappa_{-1}}{\overset{k_1}{\rightleftharpoons}}$$

$$(Na_3)E_1P \underset{\kappa_{-2}}{\overset{k_2}{\rightleftharpoons}} E_2P + 3Na_o.$$

This model extends Scheme 1 by preceding the ADP release step with a slow binding and occlusion step that equilibrates at the holding potential. Apell and Diller (26) have presented evidence that the proton-binding affinity of the E_1 conformation of the pump is significantly greater than the E_2P form and that the first two intracellular binding sites for Na^+ are occupied either by H^+ or Na^+, thereby resulting in no net charge translocation for the exchange of intracellular Na^+ and H^+ at the first two sites to be occupied before Na^+ occlusion. Since the intracellular binding site for the third Na^+ ion is located within a shallow internal access channel having a dielectric coefficient (δ_i) of ~0.25 (12), $K_m(V_h)$ is given by

$$K_m(V_h) = K_m(0)exp(-\delta_i FV_h/RT), \quad (7)$$

where $K_m(0)$ is the dissociation coefficient for binding of the third intracellular Na^+ in the absence of a membrane potential. Scheme 2 also assumes that the charge movements associated with ADP release are small and can be neglected. Since the charge available to participate in the E1–E2 conformational change and the charge translocation associated with extracellular Na^+ rebinding are limited by the slow intracellular Na^+ equilibration step, we may write the following expression for $Q(V)$ for Scheme 2:

$$Q(V) = \left[\frac{Q_{tot}}{1 + A[Na]_o^n \exp\left(\frac{-zFV}{RT}\right)} + Q_{min}\right]\left[\frac{[Na]_i}{[Na]_i + K_m(V_h)}\right]. \quad (8)$$

Note the distinction in Eq. 8 between V, the membrane potential during the test step, and V_h, the holding potential. The assumption of equilibrium binding at intracellular Na^+ sites is supported by the measurements of Heyse et al. (9), who found a forward rate constant of $1.5 \times 10^7\ s^{-1}\ M^{-1}$ and reverse rate constant of $1.64\ s^{-1}$ for the intracellular Na^+ binding step to the unphosphorylated enzyme. We may also write an expression for $Q(V)$ in the traditional form that is convenient for curve-fitting data at a fixed Na_o^+ and has one fewer free parameter:

$$Q(V) = \left[\frac{Q_{tot}}{1 + \exp\left(\frac{zF(V_q - V)}{RT}\right)} + Q_{min}\right]\left[\frac{[Na]_i}{[Na]_i + K_m(V_h)}\right]. \quad (9)$$

Since intracellular Na^+ binding that is below saturation limits the forward rate $k_1(Na_3)E_1P{\cdot}ADP$, we may write an expression for an effective forward rate coefficient (k_f) that gives its relationship to the rate coefficient k_1 that was defined for Scheme 1,

$$k_f = \frac{k_1[Na]_i}{[Na]_i + K_m(V_h)}. \quad (10)$$

The parameter k_f may be substituted for k_1 in Eq. 6, to give the following expression for the relaxation rate coefficient for Scheme 2,

$$k_{tot} = 0.5\left[k_f + \kappa_{-1} + k_2 + \kappa_{-2} - \sqrt{(k_f + \kappa_{-1} + k_2 + \kappa_{-2})^2 - 4[k_f k_2 + (k_f + \kappa_{-1})\kappa_{-2}]}\right]. \quad (11)$$

Effect of intracellular Na^+ on the amount of charge moved and its relaxation kinetics

The effect of Na_i^+ on Na_o^+-sensitive transient current was investigated at 50 mM extracellular Na^+. This concentration was selected because the midpoint voltage of the steady-state charge distribution is near the holding potential (−40 mV) at saturating Na_i^+ (50 mM, see Fig. 2 *A*). This is advantageous, since equal-magnitude voltage pulses in either the positive or the negative direction will result in approximately equal-magnitude charge transients. Examples of the effect of changes in Na_i^+ on internally perfused oocytes are shown in Fig. 3. Fig. 3, *A* and *B*, show data from an oocyte perfused with 50 mM (*open circles*) and 25 mM (*solid circles*) Na_i^+. There is a reduction both in the magnitude of the charge moved (Fig. 3 *A*) and its relaxation rate coefficient (Fig. 3 *B*) as Na_i^+ is reduced. This is made more evident in Fig. 3, *C* and *D*, obtained from a different oocyte initially perfused with 50 mM Na_i^+, followed by perfusion with 3.13 mM Na_i^+.

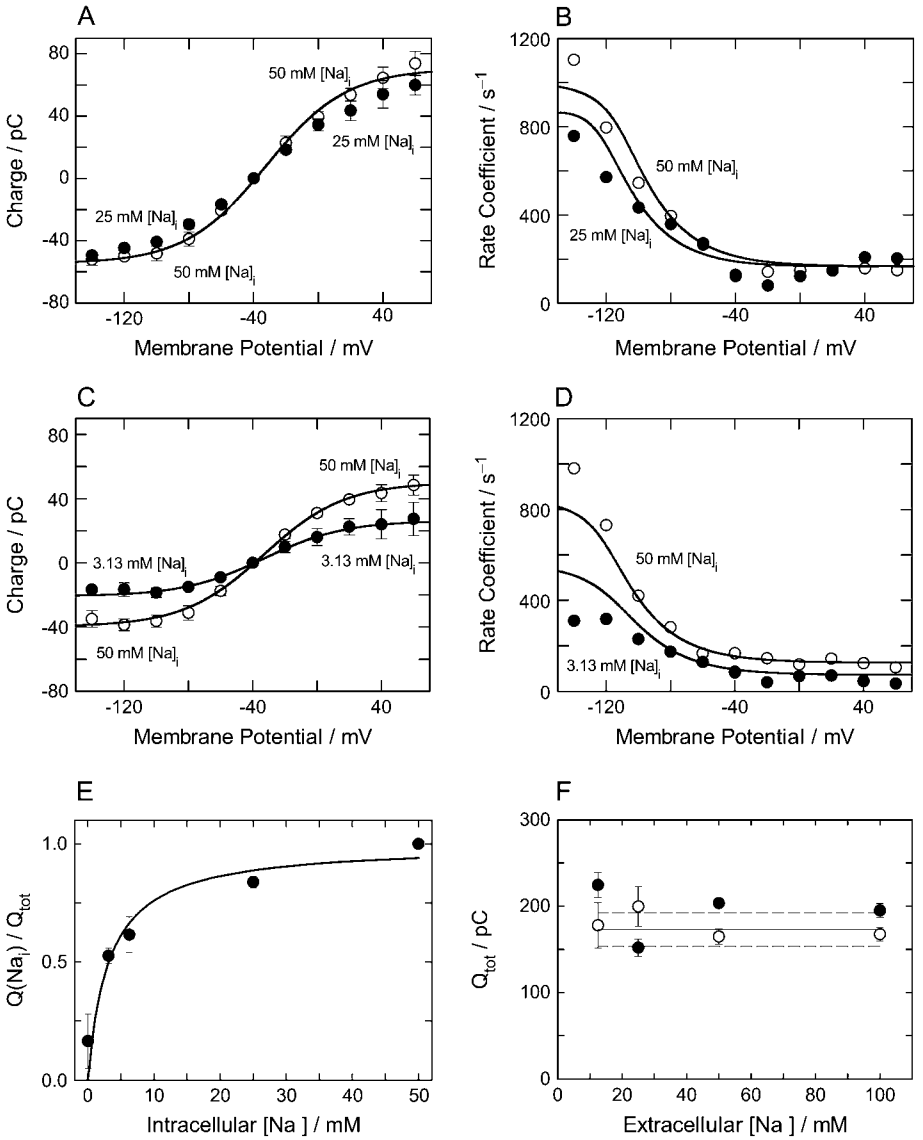

FIGURE 3 Effect of intracellular and extracellular Na^+ on Na_o^+-sensitive transient current in internally perfused oocytes. Voltage-dependence of Na_o^+-sensitive charge (*A*) and its relaxation rate coefficient (*B*) from an oocyte perfused with 50 mM (*open circles*) and 25 mM (*solid circles*) Na_i^+. Na_o^+-sensitive charge (*C*) and its relaxation rate coefficient (*D*) from a second oocyte perfused with 50 mM (*open circles*) and 3.13 mM (*solid circles*) Na_i^+. The Na_o^+-sensitive transient current at the two different Na_i^+ values in each oocyte were obtained after allowing 20 min for the perfusing solution to equilibrate at the new concentration. The data points in *A* and *C* are the mean ± SE of the on- and off-charge for each voltage pulse. The relaxation rate coefficients in *B* and *D* were measured from the on-current transient except the point at the holding potential of −40 mV, which is the mean value of the off-relaxation rate coefficient. The solid lines through the charge data represent the best fit of Eq. 8 to the data with z set equal to 1.0. The best-fit parameter values are $Q_{tot} = 153 \pm 11$ pC, $Q_{min} = -67 \pm 5$ pC, $V_q = -32 \pm 2$ mV, and $K_m(-40) = 11 \pm 3$ mM for the data in *A*; and $Q_{tot} = 95.6 \pm 1.1$ pC, $Q_{min} = -42.3 \pm 0.7$ pC, $V_q = -33 \pm 1$ mV, and $K_m(-40) = 3.23 \pm 0.16$ mM for the data in *C* at 50 mM Na_i^+. The solid lines in *B* and *D* are the best fit of Eqs. 1, 7, 10, and 11 to the data. The parameter z was set equal to 1.0, n equal to 1.47, $\kappa_{-1} = 345\ s^{-1}$, $K_m(0) = 3.2$ mM, and$\delta_i = 0.25$ The best-fit parameters are $k_1 = 880 \pm 80\ s^{-1}$, $k_2 = 250 \pm 30\ s^{-1}$, and $k_{-2} = 200 \pm 30\ s^{-1}\ M^{-1}$ for the data in *B*; and $k_1 = 770 \pm 80\ s^{-1}$, $k_2 = 180 \pm 30\ s^{-1}$, and $k_{-2} = 180 \pm 20\ s^{-1}\ M^{-1}$ for the data in *D*. (*E*) The maximum values of Q measured in 12 oocytes at the indicated Na_i^+ ($Q(Na_i)$) were normalized to the value obtained at 50 mM Na_i^+ (Q_{tot}). The solid line is the best fit of $Q(Na_i)/Q_{tot} = 1/(1 + (K_m(0)/[Na]_i))$ to the data. The best-fit value for $K_m(0)$ was 3.2 ± 0.4 mM. (*F*) Na_o^+-dependence of Q_{tot}. Open circles are the average Q_{tot} at each Na_o^+ for all of the data summarized in Fig. 2 *A*. Solid circles are values of Q_{tot} for the data from the single oocyte in Fig. 1 *B*. The solid line is the average Q_{tot} from all Q vs. V measurements over the concentration range 12.5–100 mM external Na^+ (20 measurements from seven oocytes). Dashed lines are mean ± 3 SE. Intracellular Na^+ was 50 mM in all of the experiments in *F*.

The effect of Na_i^+ on the measurable slow-charge movement is summarized in Fig. 3 *E*, which shows averaged data from 12 experiments like those in Fig. 3, *A* and *C*. For each oocyte, the available charge measured at a particular Na_i^+ ($Q(Na_i)$) was normalized with respect to the total charge measured at 50 mM Na_i^+ (Q_{tot}) in that oocyte. The solid line in Fig. 3 *E* is a one-site equilibrium occupancy (Michaelis-Menten) curve for intracellular Na^+ binding ($Q(Na_i)/Q_{tot} = [Na]_i/([Na]_i + K_m(0))$, having a least-squares value of $K_m(0)$ of 3.2 ± 0.4 mM. The interpretation is that binding of the third Na^+ to its intracellular occlusion site (26) equilibrates at a given holding potential and increases the occupancy of the phosphorylated 3 Na^+ ion-occluded state ($(Na_3)E_1P{\cdot}ADP$), thereby increasing the amount of charge available to be moved through the ADP release, conformational change, and extracellular Na^+ release steps. In contrast to the effect of Na_i^+ on the amount of charge measured, Fig. 3 *F* shows the lack of effect of Na_o^+ on Q_{tot} over the concentration range 12.5–100 mM.

Effect of intracellular Na^+ on the extracellular Na^+-sensitive transient current

Fig. 4 *A* shows the mean values of the normalized charge measured at four different Na_i^+ (50>, 25, 6.25, and 3.13 mM) from 10 experiments like (and including) those shown in Fig. 3, *A* and *C*, in which it was possible to make measurements at 50 mM Na_i^+ and at least one other concentration. In contrast to the finding that reduction of Na_o^+ produces a leftward shift of the *Q* vs. *V* curve (Figs. 1 *B* and 2 *A*) the position of the *Q* vs. *V* curve is unchanged when Na_i^+ is lowered. We interpret this to be a consequence of the fact that the transient charge movement being measured includes only extracellular Na^+-sensitive current. Scheme 2 assumes that the charge transients that are expected to result from electrogenic Na^+ binding of the third Na^+ within an internal ion-well (12,26) are not observed, because this binding step is followed by a subsequent slow occlusion step that equilibrates at the holding potential but which, in effect, isolates the intracellular binding steps from the more rapid extracellular Na^+ release steps. The least-squares fit of Eq. 2 to the normalized data with *z* set equal to 1.0 gives a value for the single free-parameter of $V_q = -36$ ± 1 mV. Fig. 4 *B* shows the mean values of the charge relaxation rate coefficients measured at these four Na_i^+. The least-squares fit to the data gave a $K_m(0)$ of 3.2 ± 0.02 mM and the additional parameters listed in the figure legend.

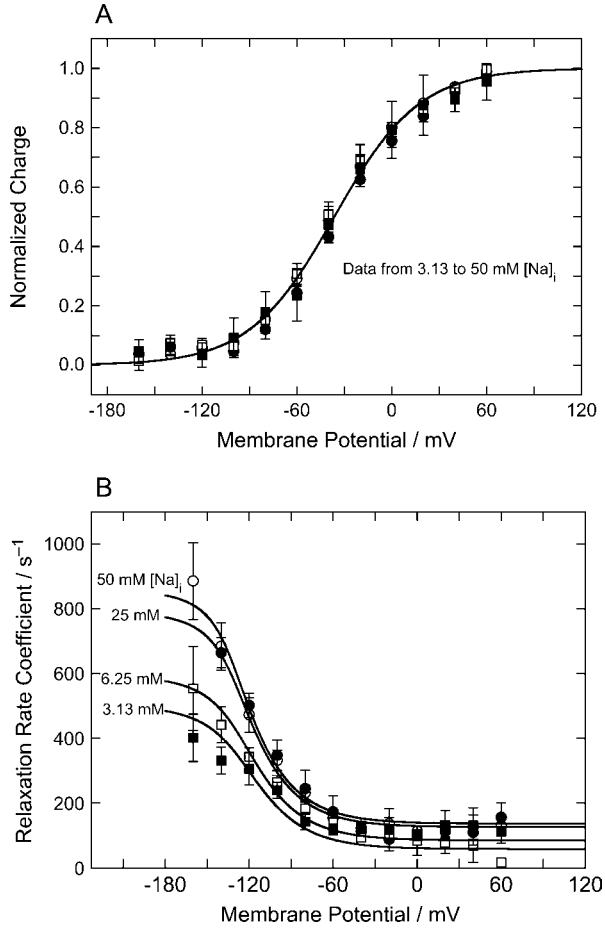

FIGURE 4 Effect of intracellular Na^+ on the voltage-dependence of extracellular Na^+-sensitive current transients. The extracellular solution contained 50 mM Na^+. (*A*) Normalized charge at an intracellular Na^+ of 50 mM (*open circles*, $n = 10$), 25 mM (*solid circles*, $n = 3$), 6.25 mM (*open squares*, $n = 6$), and 3.13 mM (*solid squares*, $n = 5$). The solid line is the best fit to Eq. 2 and gave $V_q = -36 \pm 1$ mV and $z = 0.93 \pm 0.03$. (*B*) Voltage-dependence of k_{tot} at various Na_i^+. Symbols correspond to those in *A*. Solid lines in *B* are the best fit of Eqs. 1, 7, 10, and 11 to the data. The parameter *z* was set equal to 1.0, $n = 1.47$, and $\kappa_{-1} = 345\ s^{-1}$. The best-fit parameters were $k_1 = 650 \pm 60\ s^{-1}$, $k_2 = 219 \pm 18\ s^{-1}$, $k_{-2} = 310 \pm 30\ s^{-1}\ M^{-1}$, $\delta_i = 0.22 \pm 0.12$, and $K_m(0) = 3.2 \pm 0.2$ mM.

DISCUSSION

Measurements of the dielectric coefficient for extracellular Na^+ release

The data in Fig. 2 *A* give a calculated value of $\delta = 0.69 \pm 0.02$ from the least-squares values of *z* and *n*. The equality of the shift in the midpoint voltage of the *Q* vs. *V* and k_{tot} vs. *V* curves with each doubling of Na_o^+ is strong evidence for the existence of an extracellular ion well. This value of δ (elsewhere also called λ_o) agrees with previous charge-relaxation measurements in intact *Xenopus* oocytes (2) using a two-microelectrode voltage-clamp technique (calculated to be 0.70 ± 0.04 from the observed shift of −24.8 ± 1.7 mV per doubling of Na_o^+). Gadsby et al. (25) reported a value of 0.69 ± 0.04 studying $^{22}Na^+$ unidirectional efflux mediated by electroneutral Na^+/Na^+ exchange in squid giant axon. De Weer et al. (27) measured a value of $\delta = 0.61 \pm 0.03$ in squid axon under backward-pumping conditions, and Holmgren et al. (6) measured a value of 0.71 ± 0.04 for the slow component of charge relaxation in squid giant axon. The agreement of these values is remarkably close, despite the fact that they were determined under different experimental conditions and in two different species. The fact that the external ion-well depth (δ) is a robust parameter, independent

of the intracellular [ATP] and [ADP], supports the hypothesis that it is determined only by structural considerations and represents the fractional electrical distance at which Na^+ ions are deoccluded and released to the extracellular face of the enzyme. It will be of considerable interest to determine if mutations in the vicinity of the postulated extracellular Na^+ ion egress sites (28) produce structural changes that have an effect on the profile of the electric field in this region and thereby change the value of δ.

Lack of effect of extracellular Na^+ on the magnitude of Q_{tot}

Rakowski (2) reported that increases in Na_o^+ produce an increase in the value of Q_{tot}. This effect was not predicted by the pseudo-three-state model proposed in that study. It was suggested that extracellular Na^+ is able to recruit more enzyme to participate in the slow electrogenic reactions from a nonparticipating pool. In apparent contradiction with this previous study, the data in Fig. 3 *F* show that, under Na^+/Na^+ exchange conditions (both saturating ATP and ADP present), there is no effect of Na_o^+ on the magnitude of Q_{tot}. We suggest that the postulated nonparticipating pool has been fully recruited by the presence of both ADP and ATP (29), whereas, in the intact oocytes in the previous study, the intracellular [ADP] was likely to be too low to fully activate Na^+/Na^+ exchange owing to active metabolic production of ATP from ADP.

Lack of effect of changes in intracellular Na^+ on the midpoint voltage of the *Q* vs. *V* curve

A surprising finding of these studies is the lack of effect of changes in Na_i^+ on the midpoint voltage (V_q) of the steady-state Q vs. V relationship (Fig. 4). Based on the results of others that support the presence of a shallow internal-facing ion-well having a dielectric coefficient of ~0.25 (9,11), we expected to observe a shift of the midpoint voltage of the Q vs. V curve to the right. That this effect of Na_i^+ on the Q vs. V curve was not seen can be explained by the isolation of intracellular binding steps from extracellular release steps by a relatively slow occlusion reaction, as described for Scheme 2. On the other hand, the kinetics of slow-charge relaxation were affected by changes in Na_i^+, as predicted by Eqs. 10 and 11 for Scheme 2.

The apparent valence of charge translocation (*z*) under Na^+/Na^+ exchange conditions

All of the data in this study are consistent with a value of $z = 1.0$. Initially we performed fits to the data that allowed z to be a free parameter. The mean value of z determined from these initial fits was not statistically significantly different from 1.0 ($p < 0.01$, $N = 26$). The absence of K^+ in both the internal and external solutions prevents the operation of the complete cycle of the Na^+/K^+ pump in either its forward or reverse mode. In this study, the presence of 5 mM ADP and ATP in the internal solution, and the presence of intra- and extracellular Na^+, strongly favor the operation of the Na^+/K^+ pump in its electroneutral Na^+/Na^+ exchange mode without net hydrolysis of ATP (15,16). Previous work in oocytes in the presence or absence of ADP (22) also gave values of z near 1.0. The observation that z is near 1.0 in the absence of ADP (which restricts the pump to extracellular Na^+ deocclusion and release steps) is consistent with the assumption of Scheme 2 that the slow intracellular ion occlusion step, in effect, isolates charge movement associated with intracellular Na^+ binding from the extracellular Na^+-sensitive deocclusion and release steps. This isolation provides an explanation of why neither the midpoint voltage (V_q) nor exponential steepness (z) of the transient charge are affected by changes in Na_i^+. The present study does not provide an answer to the question of whether electroneutral Na^+/Na^+ exchange is 3:3 or 1:1. Either stoichiometry could be consistent with an apparent valence (z) of 1.0.

Effect of intracellular Na^+ on the magnitude of the *Q*(*V*) relationship and the kinetics of charge relaxation

The effect of Na_i^+ on the magnitude of the $Q(V)$ relationship (Fig. 3 *E*) can be accounted for by a simple one-site binding model with a $K_m(0)$ of 3.2 ± 0.4 mM (Eqs. 7–9). The effect of Na_i^+ on the relaxation rate coefficient of pre-steady-state charge (Fig. 4 *B*) provides a second estimate (Eqs. 10 and 11) for $K_m(0)$ of 3.2 ± 0.2 mM. These values are comparable to the value of 3.6 ± 0.5 mM obtained for the highest affinity of three intracellular Na^+ sites by measurement of the activation of ATP-dependent Na^+/Na^+ exchange by cytoplasmic Na^+ in liposomes containing reconstituted shark Na^+,K^+-ATPase (30) and the value of 3 mM measured by titration by Grell et al. (31). However, as discussed by Grell et al. (31), the value of $K_m(0)$ is strongly affected by pH and the presence of other cations that effectively compete with Na^+ at its negatively charged intracellular binding sites. The close agreement may, therefore, simply be coincidental. We assume that the increase in the $Q(V)$ curves, as $[Na^+]_i$ is raised, results from production of additional 3 Na^+-occluded enzyme and the increase in the slow-charge relaxation rate coefficient results from Na_i^+ increasing the effective forward occlusion rate coefficient k_f as described by Eq. 10. The data in Figs. 2 *B* and 4 *B* do not provide strong support for the predicted saturation of the k_{tot} vs. V relationship. Greater temporal resolution of fast, medium, and slow components of charge movement will be required to examine whether the predicted saturation of the slow component can be clearly demonstrated.

Comparison of the values of the rate coefficients k_1, k_2, and k_{-2} with previous work

All of the curve-fits that require a value for the pseudo-first-order rate coefficient κ_{-1} use a value of 345 s^{-1} based on the measurement of k_{-1} of 6.89×10^4 s^{-1} M^{-1} by Peluffo (22) and the assumption that the intracellular [ADP] has a value close to that of the intracellular experimental solution (5 mM).

The rate coefficient k_1 determined here (650 ± 60 s^{-1}) falls between that of Peluffo (22) (404 s^{-1}) and that reported by Campos and Beaugé (32) (1067 s^{-1}). It is in good agreement with the value of 600 s^{-1} reported by Heyse et al. (10). Estimates of the rate coefficient k_2 vary widely, but the value determined here of 219 ± 18 s^{-1} is within the range of values measured by others (20–300 s^{-1}) in a variety of preparation using various methods. The value of k_2 reported by Peluffo (22) (130 s^{-1}) is somewhat lower. The value of the rate coefficient k_{-2} of 310 ± 30 s^{-1} M^{-1} reported here is more rapid than those found by Rakowski (2) (150 s^{-1} M^{-1}) and by Peluffo (22) (162 s^{-1} M^{-1}). The reason for this twofold discrepancy is not clear. However, the ratio k_2/k_{-2} found here (0.7 M) is close to that of Peluffo (22) (0.8 M), as expected for low affinity extracellular binding. It should be noted that these rate coefficients are thought to reflect the conformational changes associated with rate-limiting enzymatic steps involving individual Na^+ ion deocclusion/reocclusion. The diffusional translocation of ions within the postulated internal and external ion wells is faster than the temporal resolution of our measurements.

Supported by National Institutes of Health grant No. NS-22979.

REFERENCES

1. Nakao, M., and D. C. Gadsby. 1986. Voltage-dependence of Na translocation by the Na^+/K^+ pump. *Nature*. 323:628–630.
2. Rakowski, R. F. 1993. Charge movement by the Na^+/K^+ pump in *Xenopus* oocytes. *J. Gen. Physiol.* 101:117–144.
3. Holmgren, M., and R. F. Rakowski. 1994. Pre-steady-state transient currents mediated by the Na^+/K^+ pump in internally perfused *Xenopus* oocytes. *Biophys. J.* 66:912–922.
4. Rettinger, J., L. A. Vasilets, S. Elsner, and W. Schwarz. 1994. Analyzing the Na^+/K^+-pump in outside-out giant membrane patches of *Xenopus* oocytes. *In* The Sodium Pump: Structure, Mechanism, Hormonal Control and Its Role in Disease. E. Bamberg and W. Schoner, editors. Steinkopff Verlag, Darmstadt, Germany. 553–556.
5. Hilgemann, D. W. 1994. Channel-like function of the Na,K pump probed at microsecond resolution in giant membrane patches. *Science*. 263: 1429–1432.
6. Holmgren, M., J. Wagg, F. Bezanilla, R. F. Rakowski, P. De Weer, and D. C. Gadsby. 2000. Three distinct and sequential steps in the release of sodium ions by the Na^+/K^+-ATPase. *Nature*. 403:898–901.
7. Gadsby, D. C., M. Nakao, A. Bahinski, G. Nagel, and M. Suenson. 1992. Charge movements via the cardiac Na, K-ATPase. *Acta Physiol. Scand. Suppl.* 146:11–23.
8. Goldshleger, R., S. J. D. Karlish, A. Rephaeli, and W. D. Stein. 1987. The effect of membrane potential on the mammalian sodium-potassium pump reconstituted into phospholipids vesicles. *J. Physiol.* 387:331–355.
9. Or, E., R. Goldshleger, and S. J. D. Karlish. 1996. An effect of voltage on binding of Na^+ at the cytoplasmic surface of the Na^+-K^+ pump. *J. Biol. Chem.* 271:2470–2477.
10. Heyse, S., I. Wuddel, H.-J. Apell, and W. Stürmer. 1994. Partial reactions of the Na,K-ATPase: determination of rate constants. *J. Gen. Physiol.* 104:197–240.
11. Wuddel, I., and H.-J. Apell. 1995. Electrogenicity of the sodium transport pathway probed by charge pulse experiments. *Biophys. J.* 69: 909–921.
12. Domaszewicz, W., and H.-J. Apell. 1999. Binding of the third Na^+ ion to the cytoplasmic side of the Na, K-ATPase is electrogenic. *FEBS Lett.* 458:241–246.
13. Apell, H.-J. 2004. How do P-type ATPases transport ions? *Bioelectrochemistry*. 63:149–156.
14. Smith, L. D., W. Xu, and R. L. Varnold. 1991. Oogenesis and oocyte isolation. *In* Methods in Cell Biology. *Xenopus laevis*: Practical Uses in Cell and Molecular Biology. B.K. Kay and H.B. Pengs, editors. Academic Press, San Diego, CA. 45–60.
15. De Weer, P. 1970. Effects of intracellular 5′ ADP and orthophosphate on the sensitivity of sodium efflux from squid giant axon to external sodium and potassium. *J. Gen. Physiol.* 56:583–620.
16. Glynn, I. M., and J. Hoffmann. 1971. Nucleotide requirements for sodium-sodium exchange catalyzed by the sodium pump in human red cells. *J. Physiol.* 218:239–256.
17. Rakowski, R. F., L. A. Vasilets, J. La Tona, and W. Schwarz. 1991. A negative slope in the current-voltage relationship of the Na^+/K^+ pump in *Xenopus* oocytes produced by reduction of external. *J. Membr. Biol.* 121:177–187 [K^+].
18. Kimura, J., S. Miyamae, and A. Noma. 1987. Identification of sodium-calcium exchange current in single ventricular cells of guinea-pig. *J. Physiol.* 384:199–222.
19. Yang, X. C., and F. Sachs. 1989. Block of stretch-activated ion channels in *Xenopus* oocytes by gadolinium and calcium ions. *Science*. 243:1068–1071.
20. Taglialatela, M., L. Toro, and E. Stefani. 1992. Novel voltage-clamp to record small, fast currents from ion channels expressed in *Xenopus* oocytes. *Biophys. J.* 61:78–82.
21. Rakowski, R. F., A. Sagar, and M. Holmgren. 1994. Access channel model for Na^+ and K^+ translocation by the Na^+/K^+-pump. *In* The Sodium Pump: Structure, Mechanism, Hormonal Control and Its Role in Disease. E. Bamberg and W. Schoner, editors. Steinkopff Verlag, Darmstadt, Germany. 545–548.
22. Peluffo, R. D. 2004. Effect of ADP on Na^+-Na^+ exchange reaction kinetics of Na, K-ATPase. *Biophys. J.* 87:883–898.
23. Läuger, P. 1991. Electrogenic Ion Pumps. Sinauer Associates, Sunderland, MA.
24. Sagar, A., and R. F. Rakowski. 1994. Access channel model for the voltage-dependence of the forward-running Na^+/K^+ pump. *J. Gen. Physiol.* 103:869–893.
25. Gadsby, D. C., R. F. Rakowski, and P. De Weer. 1993. Extracellular access to the Na,K pump: pathway similar to ion channel. *Science*. 260:100–103.
26. Apell, H.-J., and A. Diller. 2002. Do H^+ ions obscure electrogenic Na^+ and K^+ binding in the E1 state of the Na,K-ATPase? *FEBS Lett.* 532:198–202.
27. De Weer, P., D. C. Gadsby, and R. F. Rakowski. 2001. Voltage-dependence of the apparent affinity for external Na^+ of the backward-running sodium pump. *J. Gen. Physiol.* 117:315–328.
28. Sagar, S., and R. F. Rakowski. 2003. Found: Na^+ and K^+ binding sites of the sodium pump. *News Physiol. Sci.* 18:164–168.
29. Kennedy, B. G., G. Lunn, and J. F. Hoffmann. 1986. Effects of altering the ATP/ADP ratio on pump-mediated Na/K and Na/Na exchanges in resealed human red blood cell ghosts. *J. Gen. Physiol.* 87:47–72.
30. Cornelius, F., and J. C. Skou. 1988. Non-equivalent cytoplasmic Na^+ sites and their susceptibility to transmembrane interaction from extracellular Na^+. *In* The Na^+, K^+-Pump, Part A: Molecular Aspects. J.C. Skou, J.G. Nørby, A.B. Maunsbach, and M. Esmann, editors. Alan R. Liss, New York. 485–492.
31. Grell, E., R. Warmuth, E. Lewitzki, and H. Ruf. 1991. Precision titrations to determine affinity of alkali, alkaline earth, and buffer binding to Na, K-ATPase. *In* The Sodium Pump. Recent Developments. J.H. Kaplan and P. De Weer, editors. Rockefeller University Press, New York. 441–445.
32. Campos, M. A., and L. A. Beaugé. 1997. ATP-ADP exchange reaction catalyzed by Na^+, K^+-ATPase: dephosphorylation by ADP of the E_1P enzyme form. *Biochemistry*. 36:14228–14237.